EPR study of radiation-induced defects in the thermoluminescence dating medium zircon ($ZrSiO_4$)



2002 J. Phys.: Condens. Matter 14 3813

(http://iopscience.iop.org/0953-8984/14/14/312)

INSTITUTE OF PHYSICS PUBLISHING JOURNAL OF PHYSICS: CONDENSED MATTER

J. Phys.: Condens. Matter **14** (2002) 3813–3831 PII: S0953-8984(02)31522-4

# EPR study of radiation-induced defects in the thermoluminescence dating medium zircon ($ZrSiO_4$)

**M A Laruhin, H J van Es, G R Bulka, A A Turkin, D I Vainshtein and H W den Hartog**[1]

Solid State Physics Laboratory, University of Groningen, 4 Nijenborgh, 9747 AG Groningen, The Netherlands

E-mail: h.w.den.hartog@phys.rug.nl

Received 14 December 2001, in final form 15 February 2002
Published 28 March 2002
Online at stacks.iop.org/JPhysCM/14/3813

**Abstract**

Mineral zircon has been considered as a possible medium for luminescence dating. The development of a suitable material for luminescence dating requires detailed knowledge of the processes taking place during, for example, exposure to ionizing radiation, long-term storage, annealing at moderate temperatures, excitation with (visible–UV) light. In this paper we have described our efforts to obtain relevant dating information by investigating the electron paramagnetic resonance (EPR) spectra of a variety of paramagnetic defects in mineral zircon ($ZrSiO_4$) crystals as a function of the irradiation dose, annealing time and the temperature. The rare-earth ions $Dy^{3+}$ and $Tb^{3+}$, which play a crucial role as hole traps and recombination centres, have been investigated in detail and the behaviour of the intensity of the EPR spectra associated with these impurities can be understood in terms of a theoretical model describing the luminescence related processes in zircon. In addition, a number of defects, which can be characterized by $SiO_m^{n-}$ have been identified and investigated. Also the behaviour of some of these centres has been analysed in the framework of the theoretical model.

## 1. Introduction

Zircon is a historical and well known mineral material. The word 'zircon' was mentioned for the first time in A Werner's classification as long ago as in 1782. Zircon is a widespread mineral in the world. Zircon behaves as an ionic material, the ions/molecular ions being $Zr^{4+}$ and $SiO_4^{4-}$. It is characterized by a simple crystal structure, high thermochemical resistivity, mechanical strength, and a wide variety of impurity ions—among them the rare-earth ions and several other

[1] Author to whom any correspondence should be addressed

  

transition ions can be accommodated in zircon. Therefore zircon is a very attractive medium for a variety of applications in geochronological, petrological and geochemical investigations.

The first spectroscopic studies of zircons were made in the 30's [1, 2] with optical techniques (photoluminescence, x-ray luminescence, thermoluminescence (TL), and others). The technique used in this study, electron paramagnetic resonance (EPR) is a very powerful method for investigating the detailed physical properties of paramagnetic defects in ionic materials, including natural zircon ($ZrSiO_4$). In particular, radiation-induced defects can be investigated quite effectively by means of EPR because many of these defects are paramagnetic. We are dealing with electron- or hole-centres, or in some cases it can be observed that paramagnetic defects, such as particular rare-earth ions, are transformed as a result of exposure to ionizing radiation to diamagnetic systems. EPR is an excellent method for the identification of point defects, their local environment, and kinetics of the processes involving these defects. The presence of various paramagnetic defects in natural zircon made the EPR study of the crystals complicated. Nevertheless, up to the present time zircon crystals have been studied intensively with EPR, and most of the point defects in this crystal have been identified and described.

The $Gd^{3+}$ ion was the first rare-earth ion to be studied in zircons by means of magnetic resonance [3]. The incorporation of impurities in natural and artificially grown zircon crystals has been studied in the following papers: $Er^{3+}$ [4,5] and $Dy^{3+}$ [4]; $Nd^{3+}$ and $Yb^{3+}$ [6]; $Fe^{3+}$ [7]; $Ti^{3+}$ [8, 9]; $Mn^{2+}$ [5]; $V^{4+}$ [10, 11]; $Mo^{5+}$ [12, 13]; $SiO_m^{n-}$ centres [5, 13–15]; and besides the ones mentioned here, there have been many other publications in this area.

The ultimate goal of our present efforts is to contribute to the development of a reliable TL dating method, using zircon as a medium [16], i.e. we hope to determine the age of zircon containing sediments from various geological deposits around the world. Natural zircon in particular is an interesting material for EPR investigations, because it is expected that important details of the radiation-induced defects will be revealed. In this investigation we will show that EPR is very suitable for the investigation of precisely those centres, which play a key role in the damage formation and TL processes. At this moment it appears to be essential to obtain detailed knowledge about radiation-induced defects in zircon, because from the results of our optical research we have come to the conclusion, that natural zircon is a very attractive candidate to be employed as a TL (or luminescence) dating medium. This implies that we need information about the defects which play a role in the damage formation processes and the TL (or luminescence) dating related mechanism(s).

In this work we study rare-earth (Dy and Tb) and $SiO_m^{n-}$ paramagnetic centres, which play an important role in the TL processes in many of the natural zircon samples.

## 2. Experimental procedures and results

The structure of the zircon ($ZrSiO_4$) single crystal consists of linked tetrahedra of $SiO_4$ and polyhedra $ZrO_8$. The symmetry is tetragonal with space group $D_{4h}^{19}$ ($I4_1/amd$). There are four $ZrSiO_4$ molecules per unit cell. The $ZrO_8$ polyhedra are related to each other by rotations of 90° about the $c$-axis, implying that the four substitutional $Zr^{4+}$-sites should be magnetically indistinguishable.

The EPR experiments have been carried out with a Varian 'E-line Century Series' X-band EPR spectrometer. A gas-flow helium ESR-9 'Oxford instruments' cryostat has been used to stabilize the temperature in the range of 4.2–300 K with 0.3 K accuracy. X-irradiation at room temperature has been made with an x-ray tube, with a tungsten anode, operating at 60 kV and 30 mA for several hours. A $^{137}Cs$ source was used to produce $\gamma$-irradiation at room temperature; the total dose was 10 kGy. These irradiation experiments took about 60–70 h. Much higher

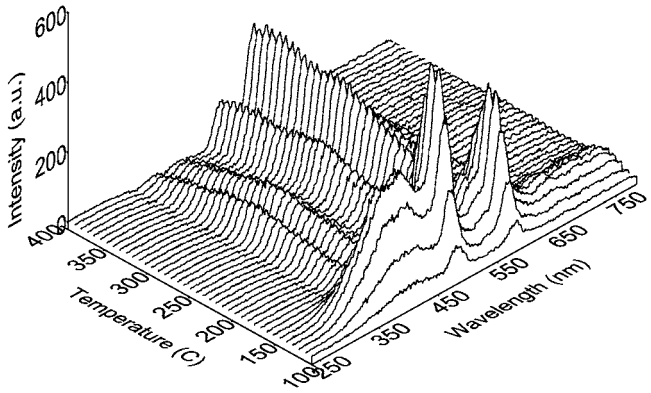


**Figure 1.** Typical TL spectrum of zircon where we can see the intense lines associated with $Dy^{3+}$ at low temperatures (i.e. 100–200 °C, $\lambda = 480$, 580 nm) and $Tb^{3+}$ at high temperatures (i.e. above 200 °C, six lines $\lambda = 375$, 416, 488, 545, 585 and 615 nm). The heating rate during the TL experiments with the DSC equipment was 150 K $min^{-1}$, or 2.5 K $s^{-1}$.

doses (up to several 100 kGy) were obtained with electrons (energy ∼0.5 MeV, maximum current ∼1 mA). For the exposure of the samples to these high-energy electrons we have used a linear electron accelerator. The dose rate for this type of irradiation experiments was very high (e.g. ∼1 MGy $h^{-1}$); therefore these irradiation runs took only a few minutes. The irradiated zircon samples were annealed isochronically in air at different temperatures up to 550 °C with 5–7 min steps using the furnace of a differential scanning calorimeter 'Perkin-Elmer DSC-7', the heating rate was 120–250 °C $min^{-1}$, and the cooling rate 250 °C $min^{-1}$.

The rare-earth impurities Dy and Tb play a dominant role in the TL of the natural zircon samples investigated in this paper. The typical TL spectrum of zircon (figure 1) consists of two sets of lines, which are associated with dysprosium (100–200 °C, $\lambda = 480$, 580 nm) and terbium (above 200 °C, six lines at $\lambda = 375$, 416, 488, 545, 585 and 615 nm) [17]. The presence of these well defined luminescence peaks shows that terbium and dysprosium ions are important luminescent recombination centres. In this paper we will discuss the radiation-induced valence changes of these ions along with the valence changes of the irradiated samples during annealing. Our results show unambiguously that $Dy^{3+}$ and $Tb^{3+}$ ions act as hole traps. From the fact that the peaks associated with dysprosium ions are located at low temperatures it should be concluded that these impurity ions are shallow hole traps. On the other hand, the terbium lines are observed at high temperatures, showing that these rare-earth ions act as deep hole traps.

EPR measurements were made on zircons single crystals and powders from different deposits: Harts Range field (Australia, monocrystals), Cambodia (monocrystals), Weld River (Tasmania, monocrystals), Tvedalen (Norway, monocrystals), Trail Ridge deposit and Green Cove Springs (Florida, USA, sand samples), Old Hickory deposit (Virginia, USA, sand samples) Ameland, the Netherlands (sand samples). At room temperature the EPR signal of $Gd^{3+}$ (figure 2) can be observed in the crystals from all deposits. Therefore we used the EPR lines of $Gd^{3+}$ for alignment of the axes of the crystalline samples with respect to the magnetic field direction. The klystron frequency was calculated from the magnetic field values of the EPR lines of $Cr^{3+}$ and $Mn^{2+}$ in a MgO reference sample, that is placed in the cavity together with the zircon samples. The $g$-values of the $Cr^{3+}$ EPR line at 300, 77, and 4.2 K are 1.978 89, 1.9782(3), and 1.9810(6), respectively.

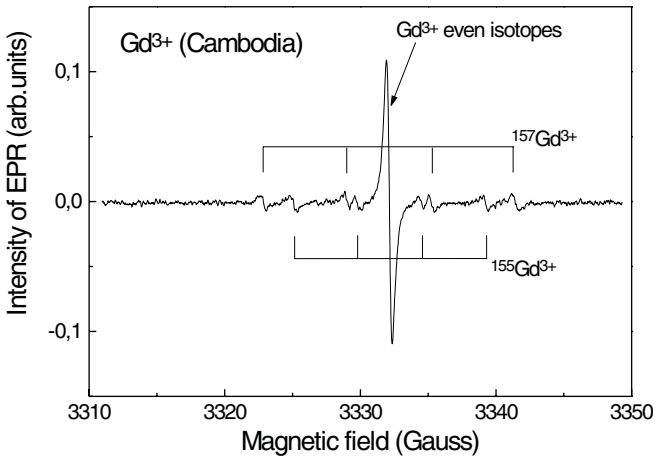


**Figure 2.** EPR spectrum of $Gd^{3+}$ ions in Cambodian zircon, with $H \parallel [001]$, measured at room temperature.

### *2.1. Anion-defects $SiO_m^{n-}$ in single crystals and powders*

As a result of the exposure to ionizing radiation some of the oxide ions in the zircon crystal structure lose an electron, which can be trapped by silicon oxide groups forming 33-electron complexes of the type $SiO_4^{5-}$, 25-electron $SiO_3^{3-}$ complexes, 17-electron $SiO_2^{-}$ complexes, and others [14, 15]. The unpaired electron (or hole) interacts with its environment. We can also expect the formation of radicals of the type $SiO_m^{n-}$ with 31, 23, 19, or 15 electrons, which all have an unpaired electron localized on the oxide ligands.

Most of the observed EPR lines of $SiO_m^{n-}$ centres in natural zircons are too weak to be identified and associated with particular (groups of) EPR lines. We have irradiated the samples with x-rays, $\gamma$- irradiation, or by an electron accelerator in order to increase the concentrations of the radiation-induced defect centres to sufficient levels to study the influence of irradiation on the defect concentration, and to study the thermostability of the centres. The typical room temperature EPR spectrum of an irradiated zircon single crystal has been presented in figure 3. For the identification of the centres we have studied the angular dependence of the EPR lines in the important crystallographic planes (figure 4). The EPR lines of the centres do not show any hyperfine or superhyperfine structure. The angular dependence of EPR lines was examined to calculate the $g$-tensor parameters. The position of one of the EPR lines does not depend on the orientation of the magnetic field; the isotropic g-factor is found to be $2.000 \pm 0.001$. This behaviour is characteristic for the $SiO_4^{5-}$ centre, which is formed during exposure of the zircon samples to ionizing radiation [15]. As the EPR line of this centre is not sensitive to rotation of the sample with respect to the magnetic field vector, the intensity of the resulting EPR line of powder is sufficient to yield information about the magnetic parameters associated with the EPR results obtained at room temperature. This property enables us to investigate these defects in zircon samples extracted from sediments, consisting of grains with typical sizes smaller than 100 $\mu$m. At room temperature the $SiO_4^{5-}$ centre is reasonably stable. A natural zircon crystal was found to contain detectable numbers of $SiO_4^{5-}$ centres and also irradiated samples showed rather intense signals due to $SiO_4^{5-}$ centres after storing the samples for 6 months in the dark. This implies that the $SiO_4^{5-}$ centre should be an important defect in our investigations connected with luminescence dating. It is uncertain yet if the $SiO_4^{5-}$ centres are sufficiently stable to allow using them as probes for dating. Much more research is needed to

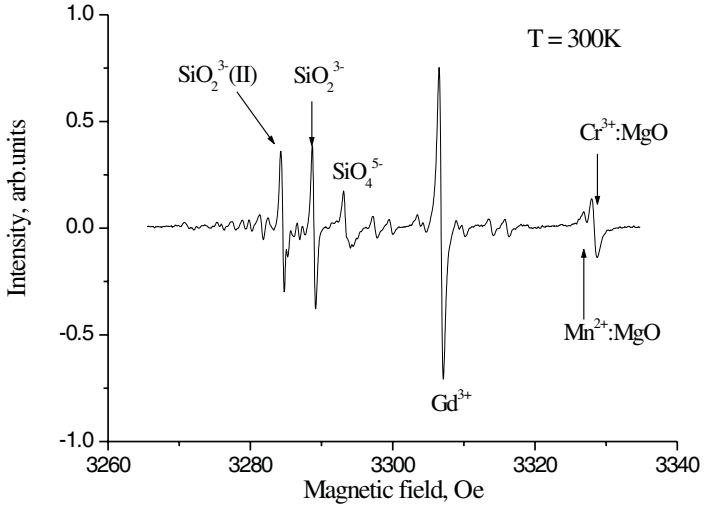


**Figure 3.** EPR spectrum of $SiO_m^{n-}$ ion-radicals (measured at room temperature) in $\gamma$-irradiated zircon single-crystal from Harts Range Fields, Australia, $H \parallel [001]$.

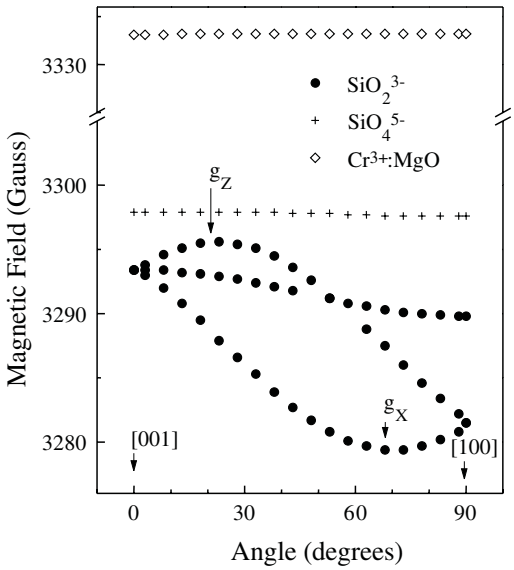


**Figure 4.** The angular dependence of the EPR lines of $SiO_2^{3-}$ and $SiO_4^{5-}$ radicals in zircon single-crystals from Harts Range fields, Central Australia.

establish the possible future role of the $SiO_4^{5-}$ centre. We note that the $SiO_4^{5-}$ centre consists of an electron trapped by a host $SiO_4^{4-}$ molecular ion, which is present in very large numbers. In this respect the $SiO_4^{5-}$ centre is different from the other centres studied in this paper. Anyway, we conclude that the kinetic properties of $SiO_4^{5-}$ centres are very important for the development of an accurate model describing the TL processes in zircon [18], because this centre will be involved in the many of the defect related and recombination reactions at moderate and high temperatures.

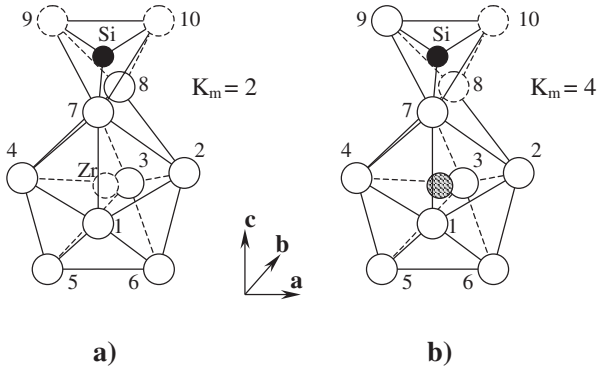


**Figure 5.** The models for (*a*) $SiO_2^-$ and (*b*) $SiO_2^{3-}$ centres in zircon. The oxygen atoms are numbered from 1 to 10. The vacancies indicated by dashed circles. Stabilization of the radicals is due to a Zr-vacancy or to some non-magnetic ion incorporated substitutionally for zirconium during crystal growth.

Another defect (labelled in this paper as '$SiO_2^{3-}$'), which appears in the crystal after exposure to ionizing radiation, shows EPR lines, which depend on the orientation of the sample with respect to the static magnetic field. For an arbitrary orientation of the sample in the magnetic field this centre shows four lines. The angular dependence of the EPR lines and the principal axes of the defect show $C_{2h}$ symmetry. The principal $g$-values are $g_X = g_Y = 2.0110$ and $g_Z = 2.0011$, the $g$-values along the crystal axes are $g_{[001]} = 2.0025$ $g_{[100]} = 2.0098$. These parameters are similar to the $g$-values of the $SiO_2^{3-} + Y^{3+}$ defect, described in [5], where the $g$-values $g_X = 2.0033$, $g_Y = 2.0076$ and $g_Z = 2.0168$ have been found. In accordance with the EPR data we conclude that the defect is a hole-type defect. EPR spectra with approximately the same structure have been found for another hole-type defect (labelled as '$SiO_2^{3-}$ (II)'). It should be noted that not in all samples $SiO_2^{3-}$ (II) centres are produced.

The models for the $SiO_2^-$ and $SiO_2^{3-}$ centres were proposed in [5]. In the present paper we do not pay attention to the 17-electron centre, because for the orientation of the magnetic field along [001] the weak lines of this defect are overlapped by Gd lines. In figure 5 we show a schematic representation of the defects, where the oxygen atoms are numbered from 1 to 10. The $SiO_2^-$ centre has been shown here to describe the nature of the defect. According to the symmetry of the EPR spectra we cannot justify the absence of the oxygen pairs 7–8 or 9–10 for the $SiO_2^{3-}$ centre, because in this case we should observe two EPR lines for arbitrary orientations of the magnetic field. The superhyperfine structure of the $SiO_2^{3-}$ defect due to the nearest Zr nucleus is not observed in the EPR spectra either. Therefore, we assume that here the stabilization of the radicals is provided by a Zr vacancy or by some non-magnetic atom (with nuclear spin zero) incorporated substitutionally for zirconium in the lattice during crystal growth.

We have found that the $SiO_2^{3-}$ hole centres are not stable at temperatures higher than 120 °C. Therefore it is interesting to study their behaviour during annealing in order to obtain information about the dynamics of shallow electron-traps in zircons.

### *2.2. The ions of rare-earth group ($Dy^{3+}$, $Tb^{4+}$)*

Rare-earth impurity ions are expected to replace the $Zr^{4+}$ ions, which are located at sites of point symmetry $D_{2d}$. Although there are four molecules per unit cell, they are all magnetically equivalent if the site remains undistorted. Trivalent rare-earth ions need charge

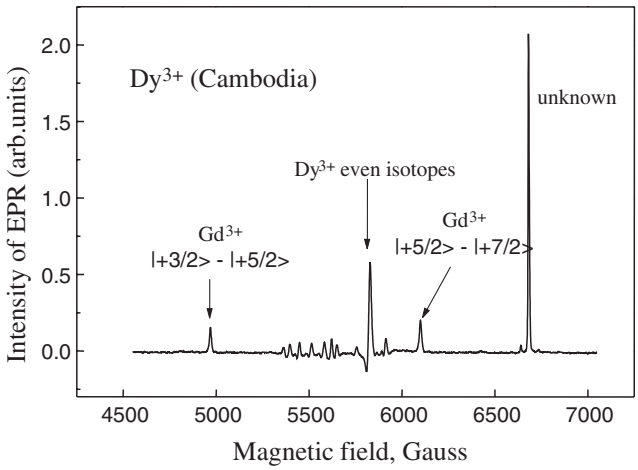


**Figure 6.** EPR spectrum of $Dy^{3+}$ from Cambodia for $H_0 \| [001]$, $T = 4$ K.

compensation to maintain charge neutrality of the crystal. Slightly doped samples (doping concentration <0.1%) exhibit mostly tetragonal spectra [6]. Once the doping is of the order of 1%, spectra of non-axial (orthorhombic) symmetry centres appear as well. The spectra associated with these centres are found to be much stronger than the tetragonal ones. As the doping concentrations in natural samples are low (in the 1–100 ppm range), this paper deals with tetragonal spectra only.

*$Dy^{3+}$.* $Dy^{3+}$ has a $4f^9$ electron configuration and a $^6H_{15/2}$ free-ion ground state. The sixteen-fold degenerate ground state with spin $J = 15/2$ is split by the tetragonal crystal field into eight Kramers' doublets. In this case the $g$-factor of the ground state must be in the range between zero and $2\lambda J = 2(4/3)15/2 = 20$ and therefore the anisotropy of the EPR spectrum will be very large. According to Rubins [19] the maximum mean $\bar{g}$ value is $\bar{g}_{max} = 2\lambda(J+1) = 7.56$. In previous EPR studies of $Dy^{3+}$ with tetragonal symmetry in various scheelite-type host crystals the values of $\bar{g} = (g_\| + 2g_\perp)/3 = 6.167$ for $CaWO_4$ [20], while for the zircon-type host $YVO_4$ it is 6.97 [21] and 6.67 for $YPO_4$ [22]. The maximum value of $\bar{g}$ was measured in zircon and its value was 7.027 [4].

Ball [4], as well as earlier authors, described the angular dependence of the EPR lines of $Dy^{3+}$ in zircon found in X- and Q-band experiments using the spin Hamiltonian ($S = 1/2$, $I = 5/2$):

$$\hat{H} = g_\| \beta H_z S_z + g_\perp \beta (H_x S_x + H_y S_y) + A S_z I_z + B(S_x I_x + S_y I_y) \tag{1}$$

with $g$-values: $g_\| = 1.132 \pm 0.001$ and $g_\perp = 9.974 \pm 0.002$. The following hyperfine constants were obtained for the isotopes $^{161}$Dy and $^{163}$Dy: $A = (0.003\,07 \pm 0.0001)\ cm^{-1}$; $B = (0.0282 \pm 0.0001)\ cm^{-1}$ and $A = (0.004\,04 \pm 0.0001)\ cm^{-1}$; $B = (0.0397 \pm 0.0001)\ cm^{-1}$, respectively. The EPR spectrum for the magnetic field orientation $H_0 \| [001]$, measured at 4 K, is given in figure 6.

We have obtained the same EPR spectra for the transparent, natural samples from Cambodia, light pink and light brown-pink pebbles from Harts Range field (Central Australia), and red-brown pebbles from Weld River (Tasmania, Australia).

We have observed an unusual broadening of the $Dy^{3+}$ EPR lines, as well as the $Gd^{3+}$ lines, which is associated with the partial, radiation-induced metamictization of the sample.

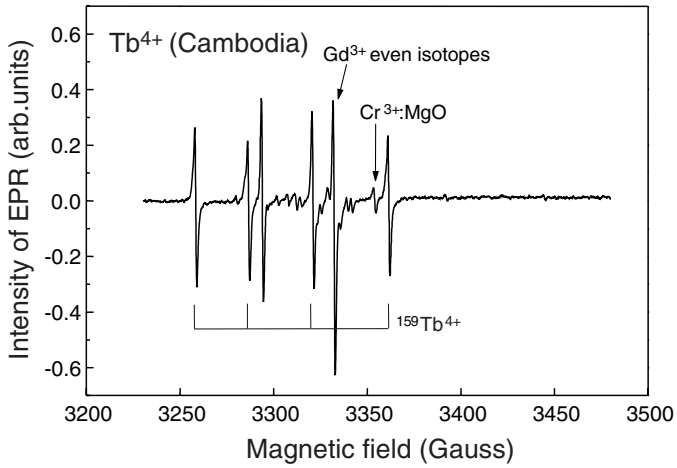


**Figure 7.** Section of EPR spectrum showing the lines associated with $Tb^{4+}$ ions in Cambodian zircon, $T = 50$ K, $H \parallel [100]$.

The $Tb^{4+}$ EPR lines associated with the transition $-1/2 \rightarrow +1/2$ should be located at about 900 G [23], and the lines of the $Dy^{3+}$ impurities with even isotopes are expected at about 660 G [4] for the orientation of $\boldsymbol{H}_0 \parallel [100]$.

*$Tb^{4+}$.* The electronic configuration $4f^7$ and the corresponding ground state $^8S_{7/2}$ of the rare-earth ions $Tb^{4+}$, $Gd^{3+}$, and $Eu^{2+}$ are easily observed by means of EPR. These high-spin state ions are perfect probes for the investigation of crystal fields (i.e. the zero field splitting (ZFS) parameters) [24]. The first studies of EPR on $Tb^{4+}$ were made for the cubic crystal structures of $ThO_2$ and $GeO_2$, where the $Tb^{4+}$ ions are situated at sites with cubic symmetry [25, 26]. The first EPR investigation of $Tb^{4+}$ ions at tetragonal sites has been carried out with zircon crystals [27]. X- and Q-band EPR spectra of synthetic zircon with 1% of Tb have been studied in the (001) crystallographic plane. The (X-band) EPR lines were observed at a magnetic field of ∼800 G (i.e. $g_{\rm eff} \approx 8$) for $H_0 \parallel [100]$, and at ∼3900 G (i.e. $g_{\rm eff} \approx 2$) for $H_0 \parallel [001]$. For the identification of the defects it was necessary to use the spin-Hamiltonian with $D_{2d}$ symmetry, including the Zeeman energy, the crystal field interaction and the super-hyperfine term, and it has the following form:

$$H = g\beta HS + \tfrac{1}{2}b_2^0 O_2^0 + \tfrac{1}{60}(b_4^0 O_4^0 + b_4^4 O_4^4) + \tfrac{1}{1260}(b_6^0 O_6^0 + b_6^4 O_6^4) + I\tilde{A}S. \quad (2)$$

Here, the $z$-axis is chosen along the crystallographic direction [001], and $x$-axis is along [100].

There are four hyperfine lines of $^{159}Tb^{4+}$ ($I = 3/2$, natural abundance 100%) with hyperfine constants (in units of $10^{-4}$ cm$^{-1}$) of $A_\parallel = 31.5 \pm 0.5$ and $A_\perp = 33 \pm 1$ (figure 7). The full set of $b_n^m$ constants has not been found, but the estimated values of the ZFS parameters were unexpectedly large as compared to the corresponding values for the isoelectronic ion $Gd^{3+}$: the second degree parameter $b_2^0 = \pm 0.769$ cm$^{-1}$ and $b_2^0 = 0.035$ cm$^{-1}$ for $Tb^{4+}$ and $Gd^{3+}$, respectively. It should be noted that the theoretical estimations of the hyperfine constants for the terbium ions with different valences have been found in [28]: $\bar{A} = 32$ G for the $4f^7$ configuration ($Tb^{4+}$); $\bar{A} = 252$ G for the $4f^8$ configuration ($Tb^{3+}$); $\bar{A} = 350$ G for the $4f^9$ configuration ($Tb^{2+}$) and $\bar{A} = 540$ G for the $4f^{10}$ configuration ($Tb^{+}$). Further EPR studies of $Tb^{4+}$ ions have been published for silicate- and germanate-type crystals: $ZrSiO_4$, $ZrGeO_4$,

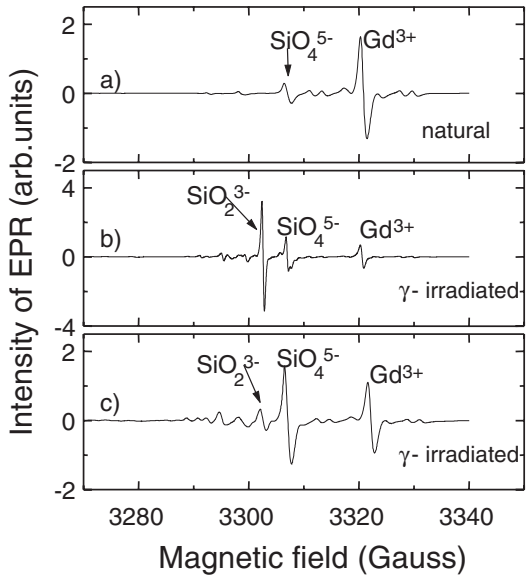


**Figure 8.** EPR spectra of pink zircon single crystals from Harts Range Field (Australia), $H \parallel [001]$. (*a*) a natural zircon single crystal without preliminary annealing; (*b*) $\gamma$-irradiated sample; (*c*) after storage in the dark for 6 months at room temperature (without any further exposure to ionizing radiation or heat treatment).

$ThSiO_4$, $ThGeO_4$, $HfSiO_4$, and $HfGeO_4$ [23]. The hyperfine splitting parameters for zircon (in units of $10^{-4}$ $cm^{-1}$) were $A_\parallel = 31.4(3)$, and $A_\perp = 33.3(3)$. It was also noted that the ZFS parameters for the above mentioned crystals are rather similar. In addition, there were no changes of the ZFS parameters and the $g$-factors as a function of the temperature in the range between 50 and 300 K: $g_\parallel = 1.999(2)$, $g_\perp = 1.989(5)$.

It should be noted that the extra, weak EPR lines in figure 7 are due to the quadrupole interactions of the type $P\{I_z^2 - 1/3I(I+1)\}$, which should be taken into account when using the spin Hamiltonian to describe the EPR results (as can be seen, this interaction has not been included in equation (2)). Natural crystals show only very weak EPR signals associated with these interactions, because the concentration of terbium ions in these materials is very low. Moreover, the EPR lines due to the $SiO_2^{3-}$, $SiO_4^{5-}$, $SiO_2^-$, $SiO_3^{3-}$ centres and the lines associated with $Gd^{3+}$, $Nb^{4+}$ and $Cr^{5+}$ are overlapping the EPR spectrum of the $^{159}Tb^{4+}$ ions for H $\parallel$ [001].

Among the investigated samples the crystal from Cambodia showed the most intense $Tb^{4+}$ EPR spectrum. The crystals from Harts Range Fields (Australia) revealed $Tb^{4+}$ EPR lines only after $\gamma$-irradiation plus a subsequent anneal in air at about $T \sim 400$ K.

### *2.3. Irradiation and annealing of zircon*

The investigation of the thermal stability of the radiation-induced paramagnetic centres was the next stage of our research. It is well known that for dating we need materials, which are capable of accumulating information about the age. In our case, zircon samples accumulate radiation induced defects formed in the crystal structure as a result of exposure to internal irradiation caused by decaying nuclei of U and Th impurities. Unfortunately, storage of the samples at room temperature leads to a decrease in the concentration of several types of defects (due to the so-called 'fading process'), therefore the problem of the thermal stability of the defects is very important and worth investigating. In figure 8 we show the EPR results for

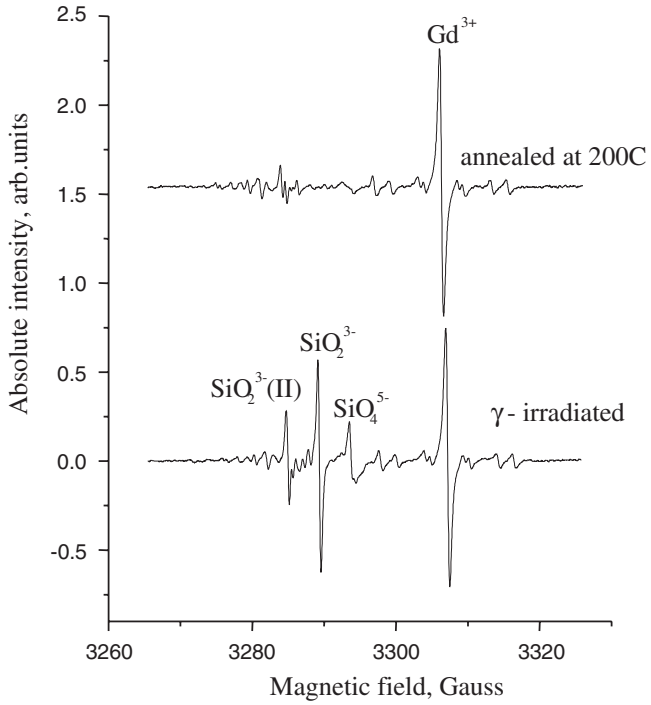


**Figure 9.** Annealing of the radiation effects in a gamma-irradiated zircon single crystal for 5 min at temperature 200 °C; during annealing the intensity of $SiO_m^{n-}$ EPR lines diminishes (the measurements have been carried out at room temperature).

(a) a natural zircon single crystal, (b) after $\gamma$-irradiation, and (c) after storage in the dark for 6 months at room temperature. The results show that in irradiated zircon significant fading takes place. The intensity of the EPR lines of the $SiO_2^{3-}$ centre increases during irradiation and it decreases when the sample is kept in the dark at room temperature. The intensity of the $SiO_4^{5-}$ centre does not decrease appreciably, i.e. this centre is reasonably stable.

The annealing experiments on the samples were made stepwise in air at increasing temperatures up to 550 °C. We have found that the $SiO_m^{n-}$ centres have a reduced stability at temperatures higher than 200 °C. Annealing of the samples for 5 min at temperature 200 °C is sufficient to diminish the EPR intensity of these defects (see figure 9). We have observed that there is a difference in stability of the two similar $SiO_2^{3-}$ and $SiO_2^{3-}$ (II) centres. The latter one is more stable than the first hole centre ($SiO_2^{3-}$).

Annealing of an irradiated zircon single crystal at temperatures >80–120 °C leads to a rapid redistribution of the electrons and holes located in shallow traps; in this process the role of the dysprosium related defects is quite obvious. In figure 10 we can see the result of this redistribution process, using the EPR spectrum of $Dy^{3+}$ as a probe, after a complete annealing run at 300 °C for 30 min. The concentration of the $Dy^{3+}$ ions decreases as a result of exposure to $\gamma$-irradiation. During subsequent annealing the intensity of the EPR signal increases again, which shows that the ion changes to either the divalent or the tetravalent state. The same behaviour is observed in crystals during exposure to irradiation from the electron accelerator (up to a total dose of 200 kGy). Subsequent annealing experiments show that the paramagnetic $Dy^{3+}$ centre is stable up to temperatures of ∼80 °C, and we propose that in the annealing/recombination process the $Dy^{3+}$ centre plays the role of a shallow hole trap.

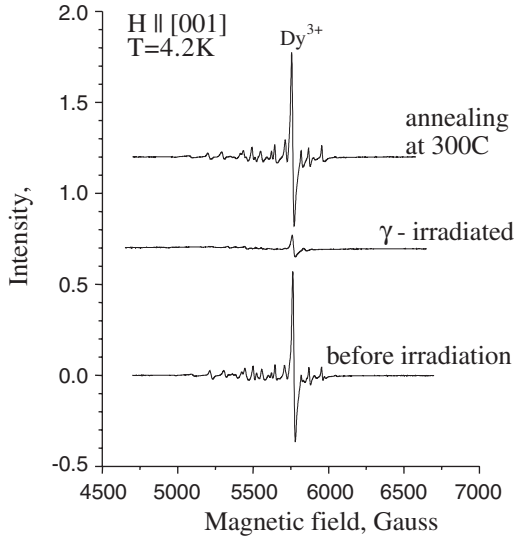


**Figure 10.** $\gamma$-irradiation of natural zircon single crystal leads to a strong reduction of the $Dy^{3+}$ EPR lines, while during subsequent annealing of the sample leads to an increase of the intensity.

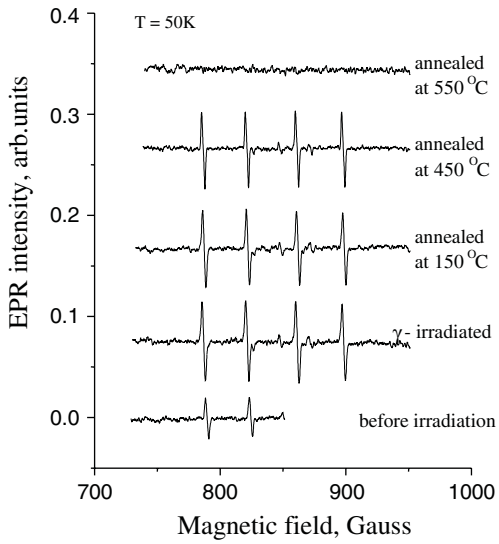


**Figure 11.** Isochronous annealing (with periods of 30 min) of a $\gamma$-irradiated zircon single crystal leads to a decrease of the intensity of $Tb^{4+}$ EPR lines.

The EPR spectra of the paramagnetic $Tb^{4+}$ centre in zircon show that this defect behaves in an opposite way as compared to $Dy^{3+}$. It should be noted, however, that this result is fully in agreement with our expectations, as will be explained below. The concentration of tetravalent terbium increases during exposure to X-, $\gamma$- or electron beam irradiation (figure 11). Subsequent annealing of the samples at high temperatures leads to a decrease of the intensity of the EPR lines of $Tb^{4+}$. The signal completely disappears at temperatures higher than 500 °C. This behaviour demonstrates that during annealing the reaction $Tb^{4+} \rightarrow Tb^{3+}$ takes place. We

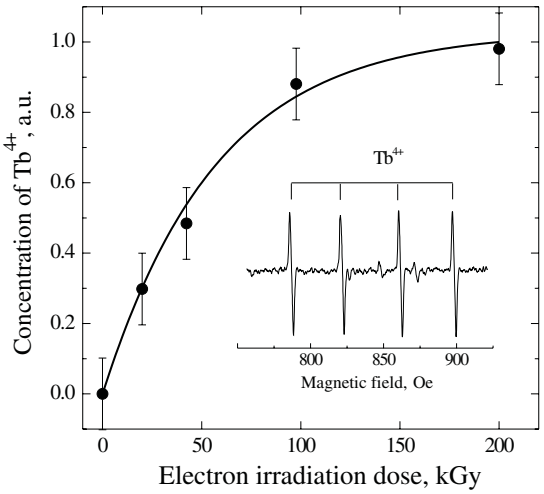


**Figure 12.** The concentration of $Tb^{4+}$ centres (which is proportional to the intensity of the corresponding EPR lines) in zircon versus the irradiation dose. The irradiation of the crystals has been carried out by a linear electron accelerator. The solid curve represents the dose dependence of the $Tb^{4+}$ concentration calculated numerically with the kinetic model described in [18].

expect a similar charge transfer behaviour for the rare-earth ions Dy and Tb, which implies that analogous to the reaction for Tb, we expect that during annealing at moderate temperatures the reaction $Dy^{4+} \rightarrow Dy^{3+}$ takes place, while during irradiation the opposite reaction $Dy^{3+} \rightarrow Dy^{4+}$ is the important one.

Irradiation and annealing of zircon single crystals do not affect the valence state of the $Gd^{3+}$ ion. We noticed changes in the structure of various defects including the centres associated with several impurities of the iron group. In this paper we do not study such transformations, but we will eventually have to take them into account in order to develop the ultimate theory of TL of zircons [18].

To develop a reliable dating method we need information about the saturation behaviour of the defect concentration as a function of the irradiation dose. For example, a typical natural zircon crystal collects an internal radiation dose from the U and Th series elements of about 10 kGy during a period of 100 000 years. Therefore, it would be interesting to know when the defect levels saturate as a function of the irradiation dose. We have irradiated the same zircon monocrystal up to different doses using the electron accelerator. After each step we completely annealed the sample at $T = 550\,^{\circ}\mathrm{C}$, to bring the system back to the initial state. As one can see (figure 12), the saturation of terbium energy levels starts at a dose $D \sim 50$–$100$ kGy. The solid line represents the theoretically calculated dose dependence of the $Tb^{4+}$ concentration in zircon. The kinetic model, discussed elsewhere [18], has been used to simulate the processes taking place at the different stages relevant to thermoluminescent dating. With this model it is also possible to simulate the evolution of the tetra-valent terbium ions during exposure to ionizing radiation and fading or annealing at moderate temperatures. In the model we take into account the fact that in real materials the levels associated with electron and hole traps are distributed over a wide energy interval. Various trapping and re-trapping processes, effects of redistribution of charge carriers over the available traps as well recombination reactions between electrons and holes are naturally included in the model, implying that with this model we are able to describe realistically the processes taking place during the excitation stage, i.e. during exposure to ionizing radiation. It is assumed in these model calculations that the dose

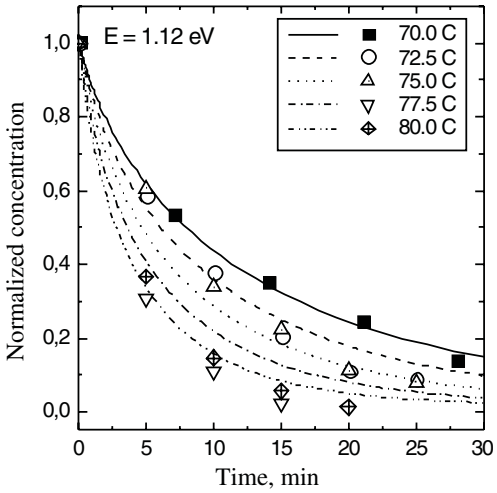


**Figure 13.** The dependence of the $SiO_2^{3-}$ centre EPR intensity, which is proportional to the concentration, versus the annealing time. Symbols indicate EPR intensity measured experimentally. Curves correspond to the theoretically calculated concentration of filled hole traps with $E = 1.12$ eV.

rate of the electron accelerator, which is 13 kGy $min^{-1}$, corresponds to a production rate of electron–hole pairs equal to $10^{-6}$ $s^{-1}$ per zircon lattice site. We observe that the concentration of $Tb^{4+}$ centres, i.e. a hole trapped at a $Tb^{3+}$-centre, shows some tendency to saturate for high irradiation doses. We note that the saturation behaviour depends on the dose rate. For the above mentioned dose rate (for electron irradiation) the maximum value of the filled traps was found to be about 60% of the total number of available terbium centres.

### *2.4. Kinetics of the centres in zircon*

For the evaluation of the parameters, which are relevant for the kinetics of the centres studied in this paper, we have performed a series of the annealing experiments for some of the paramagnetic centres at different temperatures.

We have observed that the $SiO_2^{3-}$ centre is the least stable one. It completely disappeared during annealing at temperatures above 100–120 °C. In figure 13 we show the dependence of the $SiO_2^{3-}$ centre EPR intensity versus the annealing time, observed for annealing experiments carried out between 70 and 80 °C. The annealing behaviour of these centres cannot be described by a simple exponential law corresponding to one shallow trap. This means that there are different centres involved in the annealing processes or we are dealing with a distribution of paramagnetic defects within the temperature interval 80–120 °C. We need an advanced theoretical model to explain the annealing results for the $SiO_2^{3-}$ defect, since the behaviour of the different electron- and hole-centres is coupled strongly, and the excitation of electron–hole pairs, trapping of free electrons and holes, redistribution of electrons and holes over the available traps by ionization and subsequent re-trapping and recombination processes occur simultaneously. In fact, the situation in zircon is quite complex, because we have to take into account the effects of at least three types of hole traps and many different electron traps with a wide range of trap depths. The model, which has been developed by Turkin *et al* [18] to explain the phenomena related to TL of zircon, has been used here to explain the experimentally observed annealing results for the $SiO_2^{3-}$ centre, which have been presented in figure 13. The

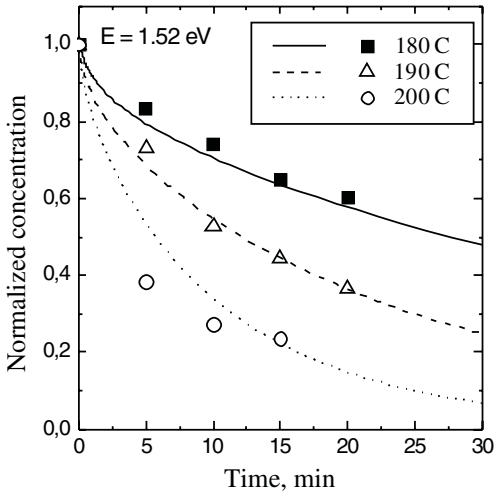


**Figure 14.** The dependence of the $SiO_2^{3-}$ (II) centre EPR intensity, which is proportional to the concentration, versus the annealing time. Symbols indicate EPR intensity measured experimentally. Curves correspond to the theoretically calculated concentration of filled hole traps with $E = 1.52$ eV.

curves in figure 13 represent the best fits of the model calculations to the experimental data points.

It should be noted that recombination of the $SiO_2^{3-}$ centre depends strongly on the origin of the sample. Moreover similar samples from the same bulk single crystal showed different intensities for the EPR lines (up to 20%). In the beginning we could obtain only crude estimates with a one-exponential process; in this case the activation energy $E_a$ for the $SiO_2^{3-}$ centre was estimated to be $1.0 \pm 0.4$ eV. The theoretical model calculations for the time dependence of the concentration of hole traps with $E_a = 1.12$ eV yield a good fit to our experimental data. The model parameters used here to explain the annealing results are the same as those used for figure 12 to simulate the EPR observations for the $Tb^{4+}$ centres after electron irradiation at a very high dose rate. Again, it should be emphasized that the annealing curves represent the behaviour of the trap system as a whole for the zircon sample, rather than the detrapping of holes from traps of single type. For a complex defect system such as natural zircon one can hardly expect to observe a simple exponential annealing behaviour.

The $SiO_2^{3-}$(II) centre is more stable than the $SiO_2^{3-}$ centre. We have studied the kinetic properties of the EPR signal of the $SiO_2^{3-}$(II) centre in zircon single crystals. In figure 14 one can see the dependence of the EPR intensity associated with the $SiO_2^{3-}$(II) centre versus time for different annealing temperatures (180, 190 and 200 °C). This behaviour is similar to that observed for the $SiO_2^{3-}$ centre, although it clearly demonstrates the higher stability of the centre investigated here. In the present case of radiation effects in natural zircon, we are dealing with a multitude of defects showing a variety of activation energies. The electron traps show a rather wide distribution of activation energies, which has been taken into account to explain the observed features of the defect system. The theoretical simulations of the kinetics of the $SiO_2^{3-}$(II) hole-type centre show that the activation energy (i.e. the trap depth) of this defect is 1.52 eV.

The experimental work on the rare-earth centres was time consuming, because it was necessary to study the defects corresponding with the different annealing stages with EPR at low temperatures. In figure 15 we show the time dependence of the intensity of the EPR signal

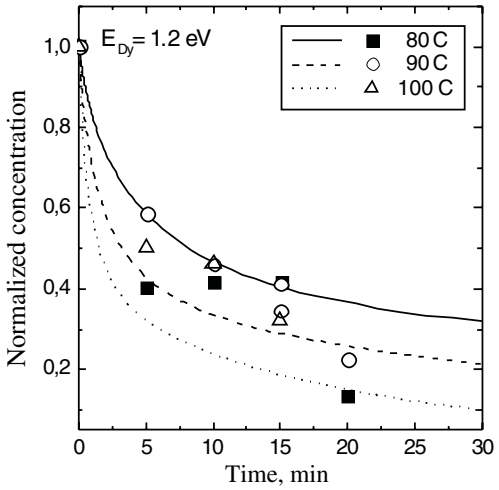


**Figure 15.** The dependence of the dysprosium concentration (symbols indicate intensity $I = I_{EPRmax} - I_{EPR}$ of $Dy^{3+}$ EPR lines) versus the annealing time. Curves correspond to the theoretically calculated concentraiton of $Dy^{4+}$ centers with $E = 1.2$ eV.

for the $Dy^{3+}$ centre. Here too, the decay curves do not behave according to a one-exponential theory. With the advanced theoretical model mentioned above [18] we calculate an activation energy of ∼1.2 eV, which means that at about 100 °C the dysprosium impurities play the role of shallow hole traps.

A different behaviour is found by measuring the properties of the EPR signal of the $Tb^{4+}$ centre. This centre does not show a well defined decay behaviour. The EPR intensity starts to decrease at about $T \sim 300$ °C, but after annealing at much higher temperatures, even up to ∼450 °C the signal was still present to some extent. The only explanation for this behaviour, that we can provide, is that the $Tb^{4+}$ ion is a very deep hole trap and the decrease of the luminescence intensity is caused by recombination with electrons released from traps filled with electrons. This means that we cannot measure activation energy $E_a$ of the paramagnetic $Tb^{4+}$ centre itself. We are able to obtain only some effective activation energy $E_{a,\mathrm{eff}}$ of the annealing process, which depends almost completely on the kinetics of many other centres in the crystal.

## 3. Discussion

We have investigated in this paper several paramagnetic defects in irradiated natural zircon crystals from a variety of geological localities around the world. As mentioned above, our efforts are aimed at the development of methods to date geological samples by means of luminescence techniques. Therefore we have focused our attention at the defects, which play a role in the TL phenomena of natural zircon investigated after exposure to artificial irradiation in our laboratory [16]. The most obvious features of the TL results are the spectral components produced by two rare-earth ions, $Dy^{3+}$ and $Tb^{3+}$. In addition, there is another contribution, which is not due to rare earth impurities and can (probably) be explained in terms of a host emission of the zircon crystal.

Although there are many types of rare-earth impurities present in natural zircon, only two of them contribute to the TL signal. An interesting feature of natural zircon crystals is

that they usually contain sufficient concentrations of trivalent Gd, which is paramagnetic (the $^8S_{7/2}$ state) and shows a relatively strong EPR signal in a wide range of temperatures, including room temperature. This property is very useful for the purpose of obtaining a precise orientation of the crystallographic axes of the sample with respect to the external static magnetic field. The presence of this signal has helped us to find the locations of the EPR lines of the radiation-induced centres and define the principal values of the magnetic parameters of the associated defects.

The first important group of radiation-induced defects in natural zircon can be characterized by the formula $SiO_m^{-n}$. Depending on the values of the integers $n$ and $m$ we are dealing with electron- or hole-centres. The most important electron-centre is the defect, which can be represented by $SiO_4^{5-}$. This defect is produced readily during exposure to ionizing radiation, and it is moderately stable during storage in the dark at room temperature, which implies that the unpaired electron associated with the EPR signal plays a role in the phenomena of trapping, re-trapping and recombination. During storage at room temperature the trapped electron has a non-zero probability to be released. From there it may:

(i) travel in the conduction band until it is re-trapped by the same type of ionized centre, trapped at another location (redistribution of the electrons over the available trapping sites) or
(ii) the electron recombines with a hole-centre, which may give rise to the emission of a quantum of light (luminescence) or it could induce a radiationless recombination event.

On the other hand the $SiO_4^{5-}$ centre is quite useful for investigating the defect state of natural zircon immediately after the exposure to laboratory irradiation by means of EPR. The EPR line associated with this defect can be observed at room temperature, and the signal is isotropic. As a result of this property, one can detect the centre very effectively in single crystals as well as in powders. This means, that the $SiO_4^{5-}$ centre can be measured very easily for single crystals with random orientations and concentrates of zircon from sediment samples. For dating purposes, we are interested primarily in electrons or holes in deep traps. It might be that the $SiO_4^{5-}$ centre is not a defect, which can be ideally used in dating experiments. On the other hand, we have observed significant concentrations of $SiO_4^{5-}$ centres in natural and faded samples. As mentioned above, we should take into account the fact that some of the electrons released from these shallow traps will be re-trapped in the deeper traps, which are sufficiently stable for application as a dating defect. More research in this area is needed to draw final conclusions about the possible role of the $SiO_4^{5-}$ centre in dating natural zircon.

One of the important hole centres in zircon is the defect, which can be represented by $SiO_2^{3-}$ molecules. The $SiO_2^-$ centre is known as the 17-electron centre, where probably one electron is located near the Si atom. It is an electron centre, analogous to for example the $[CO_2]^-$ centre. It has $K_m = 2$, where $K_m$ is a number of magnetically inequivalent sites, i.e. there are in general two lines in EPR and the symmetry of the defect is $C_{2v}$.

The $[SiO_2]^{3-}$ centre is a 19-electron centre. In general, we observe four lines, which means that $K_m = 4$. Accordingly it has a different type of symmetry. It means that the model we suggested before (two O vacancies together with the vacancy of Zr along the $c$-axis) is not correct. In fact we should see with EPR two lines for arbitrary orientations of the static magnetic field with respect to the crystal axes (i.e. $K_m = 2$). So we have a defect centre with two O vacancies (only one of them is the closest one to the Zr site), together with a Zr ion, which is replaced by a non-paramagnetic ion (because we do not see any superhyperfine structure from the Zr nucleus).

We will now discuss the results obtained for the radiation-induced concentration changes of paramagnetic impurities. Trivalent gadolinium ions are not in this category, because these

ions are present in all natural zircon samples, i.e. in non-irradiated natural zircon, in irradiated and in annealed samples and they are not affected by ionizing radiation. This suggests that the trivalent state is highly stable, which is not unexpected, because the $Gd^{3+}$ ion has a half filled 4f shell and the electronic configuration is $4f^7$ (or $^8S_{7/2}$). In addition, we have observed in several samples the EPR signal of trivalent dysprosium. These ions are present in particular in annealed samples. In fact, the signal of $Dy^{3+}$ ions is reduced during exposure to ionizing radiation and we have found that ultimately the signal disappears for very high doses of irradiation. The most likely explanation for these observations is that during exposure to ionizing radiation the dysprosium impurities in the zircon crystal lattice change to the tetravalent state. After exposure to high doses all Dy-ions are in the tetravalent state and the EPR signal associated with $Dy^{3+}$ has disappeared. This result implies that the decreasing numbers of trivalent dysprosium provide information about the acquired dose.

From the point of view of luminescence dating the behaviour of the terbium impurities is most interesting, because as mentioned above the TL light at high temperatures is predominantly due to terbium impurities. Our results show that the EPR signal associated with tetravalent terbium increases gradually with increasing dose, showing a tendency to saturate at very high doses ($D > 100$ kGy, see figure 12). In annealed zircon samples the EPR signal of the paramagnetic defect associated with $Tb^{4+}$ cannot be observed, suggesting that the terbium ions are all in the trivalent state. After exposure to ionizing radiation we observe an EPR pattern, which is due to $Tb^{4+}$; this conclusion is drawn on the basis of the positions of the EPR spectrum and from the fact that the four-lines hyperfine structure including the observed splitting is typical for the interaction of the $4f^7$ electron system with the $^{159}$Tb nucleus. It should be noted here that the results for Tb and Dy are consistent, because in both cases it appears, that in non-irradiated or annealed zircon samples these impurities are in the trivalent state. Unfortunately, only $Tb^{4+}$ and $Dy^{3+}$can be observed by means of EPR (and not $Tb^{3+}$and $Dy^{4+}$), which implies that during irradiation we can only probe the production of the radiation-induced $Tb^{4+}$ ions, while for Dy we can only investigate the radiation-induced reduction of the concentration of the $Dy^{3+}$ ions.

## 4. Concluding remarks

We have investigated the properties of the EPR spectra of several radiation-induced, paramagnetic defects in a variety of natural zircon crystals. From the point of view of luminescence dating in particular the defects associated with Dy and Tb impurities are considered to be important, because they are the main luminescence activators in zircon. The EPR investigations of the Dy and Tb impurities have provided us with complementary information, because in unirradiated zircon we can study the existing paramagnetic trivalent Dy centres, which are transformed into tetravalent ions (not observable in EPR). Oppositely, the trivalent terbium ions cannot be observed in EPR, while the tetravalent can be measured conveniently. This implies that the radiation induced change of the valencies of two important rare-earth ions can be detected.

The rare-earth impurities $Dy^{3+}$ and $Tb^{4+}$ have been investigated in detail and it was possible to explain the behaviour of the EPR signal of these defects as a function of the irradiation dose and the annealing conditions (temperature and time) in terms of a theoretical model, which has been developed in [18] to understand the luminescence dating related phenomena in zircon. The results allowed us to probe the $Tb^{3+} \leftrightarrow Tb^{4+}$ transformation during irradiation and it immediately shows that the Tb ions play the role of deep hole traps in zircon. $Dy^{3+}$ centres also play a role as a hole trap, but this one is shallow. These developments are very important in our efforts to show that it is possible to use natural zircon for luminescence dating, because

we have found a possibility to unravel some of the detailed processes in TL dating. It is expected that with this new information the above mentioned theoretical model can be tested and improved and ultimately this model (or a further modifiation) is seen to be one of the key elements in future luminescence dating techniques. It has been shown that external electron irradiation up to 100 kGy does not saturate energy levels of $Tb^{4+}$ centres, which suggests that in principle the TL dating method with zircon can be applied to sediments with a wide range of ages, possibly several hundred thousand years.

In addition, the role of several $SiO_m^{n-}$centres has been studied. The behaviour of the $SiO_m^{n-}$centres in irradiated zircon during particular treatments has provided important new information, which can be used in the further investigations to develop a dependable luminescence dating method for natural zircon. It has been shown that also the behaviour of the $SiO_m^{n-}$centres can be understood quite well, although it will be necessary to collect more information about the different types of this category of defects. The thermal stability of the $SiO_2^{3-}$ and $SiO_2^{3-}$ (II) centres has been investigated, the latter centre being the more stable one. We have concluded that several types of $SiO_m^{n-}$centres play the role of shallow traps in naturally and artificially irradiated zircon samples. Especially the properties of the $SiO_4^{5-}$ centre are interesting, because

(i) they appear to be produced as a result of electron trapping by highly abundant host molecular ions of the type $SiO_4^{4-}$,
(ii) the stability properties seem to be relatively favourable,
(iii) these defects have been observed in natural zircon samples from the Trail Ridge deposit (i.e. no additional irradiation dose) and faded ones, and (iv) the EPR spectrum is isotropic, which implies that the EPR lines can also be detected conveniently for sand samples, or powdered material.

The results obtained from the EPR results obtained in this paper turned out to be very useful for our overall understanding of the kinetics of radiation-induced defect centres in zircon crystals and powders and will provide decisive information necessary for the development of models to describe the TL properties of natural zircon samples.

## Acknowledgments

This research is supported by the Dutch Technology Foundation STW, Applied Science Division of NWO and the Technology Programme of the Dutch Ministry of Economic Affairs, project GNS.4132.

## References

[1] Haberlandt H 1934 *S.-Ber. Akad. Wiss. Wien. Ser. IIa* **143** 11
[2] Lietz J 1937 *Z. Kristallogr.* **97** 337
[3] Hutton D R and Troup G J 1964 *Br. J. Appl. Phys.* **15** 405
[4] Ball D 1971 *Phys. Status Solidi* b **46** 635
[5] Nizamutdinov N M 1976 *PhD Thesis* Kazan State University, Russia p 180 (in Russian)
[6] Ball D 1982 *Phys. Status Solidi* a **111** 311
[7] Ball D 2000 *Phys. Status Solidi* b **218** 545
[8] Solntsev V P and Shcherbakova M Ya 1972 *Z. Strukt. Khim.* **13** 924 (Engl. transl. 1972 *J. Struct. Chem.* **13** 859)
[9] Claridge R, McGavin D G and Tennant W C 1995 *J. Phys.: Condens. Matter* **7** 9049
Claridge R, Lees N S, Tennant W C and Walsby C J 1999 *J. Phys. C: Solid State Phys.* **11** 3571
[10] Ball D and Wanklyn B M 1976 *Phys. Status Solidi* a **36** 307
[11] Di-Gregorio S, Greenblatt M, Pifer J H and Sturge M D 1982 *J. Chem. Phys.* **76** 2931
[12] Eftaxias K, Fielding P E and Lehmann G 1989 *Chem. Phys. Lett.* **160** 36

[13] Krasnobaev A A, Votyakov S L and Krohalev V Ya 1988 *Spectroscopy of Zircons* (Moscow: Science) (in Russian) ISBN-5-02-002618-2 pp 150
[14] Barker P R and Hutton D R 1973 *Phys. Status Solidi* b **60** K109
[15] Solntsev V P, Shcherbakova M Ya and Dvornikov E V 1974 *J. Struct. Chem.* **15** 217
[16] van Es H J, den Hartog H W, de Meijer R J, Venema L B, Donoghue J F and Rozendaal A 2000 *Radiat. Meas.* **32** 819
[17] Iacconi P and Caruba R 1980 *Phys. Status Solidi* **62** 589
[18] Turkin A A, van Es H J, Vainshtein D I and den Hartog H W A kinetic model of zircon thermoluminescence *Nucl. Instrum. Methods* B at press
[19] Rubins R S 1970 *Phys. Rev.* B **1** 139
[20] Antipin A A, Kurkin I N, Potvorova L Z, and Shekun L Ya 1965 *Fiz. Tverd. Tela* **7** 3685 (Engl. transl. 1966 *Sov. Phys.–Solid State* **7** 2979)
[21] Ranon U 1968 *Phys. Lett.* A **28** 228
[22] Ranon U, Danner J C and Stamires D N 1968 *Bull. Am. Phys. Sjc.* **13** 1671
[23] Hansen S, Mosel B D, Müller-Warmuth W and Fielding P E 1996 *Z. Naturforsch.* A **51** 885
[24] Abraham M M and Bleaney B 1970 *Electron Paramagnetic Resonance of Transition Ions* (Oxford: Clarendon)
[25] Baker J M, Chadwick G R, Garton G and Aurell G P 1965 *Proc. R. Soc.* A **286** 352
[26] Greznev Y S, Zaripov M M and Stepanov V G 1966 *Sov. Phys.–Solid State* **7** 2937
[27] Hutton D R and Melhe R J 1969 *J. Phys. C: Solid State Phys.* **2** 2297
[28] Abdous A and Baker J M 1977 *J. Phys. C: Solid State Phys.* **10** 4837